Electronic Supplementary Material (ESI) for Analyst
This journal is © The Royal Society of Chemistry 2019

Electronic Supplementary Information

A simple hypochlorous acid signaling probe based on resorufin carbonodithioate and its biological application

Myung Gil Choi, Yu Jeong Lee, Kang Min Lee, Kyoung Yeol Park, Tae Jung Park* and Suk-Kyu Chang*
Department of Chemistry, Chung-Ang University, Seoul 06974, Republic of Korea

Contents

Table S1. Comparison of representative HOCl-selective optical signaling probes

Structure	Signaling	Sensing mechanism	Condition	Limit of detection	Application	Reference
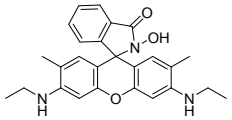	Colorimetry, Fluorescence	Oxidative hydrolysis of hydroxamic acid	PBS buffer-DMF (0.1%) at pH 7.4	< 25 nM	Visualization of HOCl in A549 cells and zebrafish	[1]
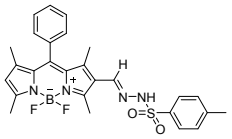	Colorimetry, Fluorescence	Oxidative hydrolysis of sulfonhydrazone	PBS buffer (pH 7.4, 10 mM) and EtOH (1 : 1, v/v)	7.5 nM	Visualization of HOCl in HeLa and RAW 264.7 cells	[2]
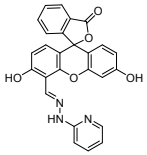	Colorimetry, Fluorescence	Oxidative hydrolysis of hydrazone	PBS buffer (pH 7.4)	7.5 nM	Visualization of HOCl in RAW 264.7 cells	[3]
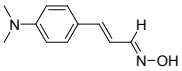	Colorimetry, Fluorescence	Formation of isoxazoline	PBS buffer (pH 7.4)	163 nM	Visualization of HOCl in C6 glial and BV2 cells	[4]
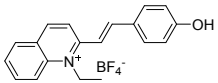	Colorimetry, Fluorescence	Oxidative hydrolysis of boronic acid	NaH_2PO_4-Na_2HPO_4 buffer (pH 7.4)	63 nM	Determination of HOCl using probe coated test paper	[5]
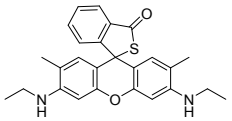	Fluorescence	Desulfurization of thiolactam	KH_2PO_4 buffer (pH 5.5) containing 1% CH_3CN	-	Visualization of HOCl in human polymorphonuclear neutrophils and intestinal epithelia of Drosophila	[6]

Table S1. Comparison of representative HOCl-selective signaling probes (*continue*)

Structure	Signaling	Sensing mechanism	Condition	Limit of detection	Application	Reference
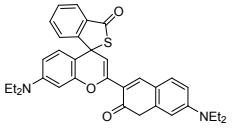	Colorimetry, Fluorescence	Desulfurization of thiolactam	PBS buffer (20 mM, pH 7.4) with 30% CH_3CN	40 nM	Determination of HOCl in tap water and visualization of HeLa cells	[7]
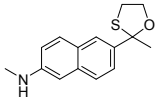	Fluorescence	Oxidative hydrolysis of oxathiolane	PBS/EtOH (1:1, pH 7.4)	16.6 nM	Visualization of HOCl in mitochondria of HeLa cells	[8]
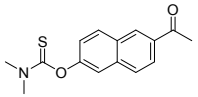	Fluorescence	Oxidative hydrolysis of thiocarbamate	PBS buffer (pH 7.4)	2.37 nM	Visualization of HOCl in HeLa, 4T1, and RAW 264.7 cells	[9]
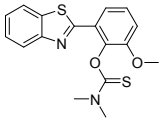	Fluorescence	Oxidative hydrolysis of thiocarbamate	PBS pH 7.4, containing 1% DMSO	0.16 nM	Visualization of HOCl in HeLa cells	[10]
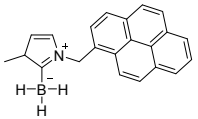	Fluorescence	Oxidative hydrolysis of *N*-heterocyclic carbene borane	PBS (pH 7.4)	-	Visualization of HOCl in RAW 264.7 cells and hippocampal slice	[11]
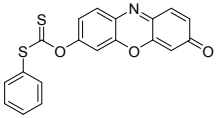	Colorimetry, Fluorescence	Oxidative hydrolysis of carbonodithioate	Phosphate buffer (pH 7.4) containing 1% CH_3CN	2.1 nM	Visualization of HOCl in RAW 264.7 and HeLa cells	This work

(a)

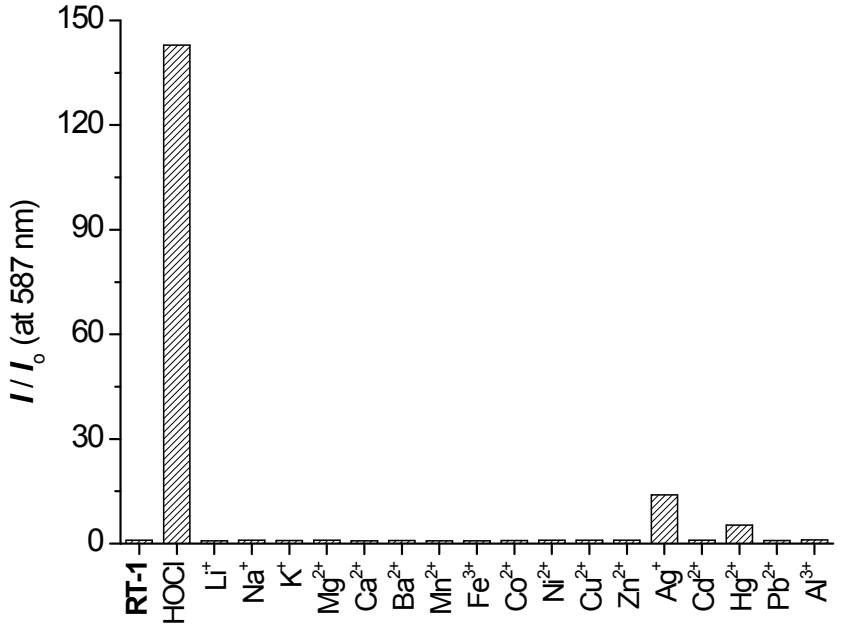

(b)

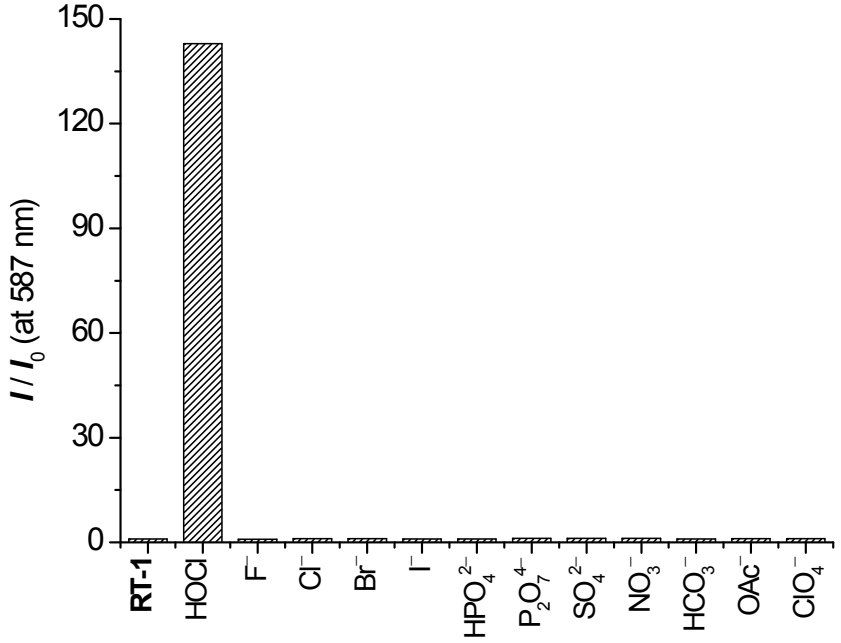

Fig. S1. Changes in fluorescence intensity of **RT-1** at 587 nm (I/I_o) in the presence of (a) common metal ions and (b) anions. [**RT-1**] = 5.0×10^{-6} M, [HOCl] = 2.5×10^{-5} M, [M^{n+}] = [A^{n-}] = 5.0×10^{-5} M in phosphate buffer solution (pH 7.4) containing 1% (*v/v*) acetonitrile, λ_{ex} = 550 nm.

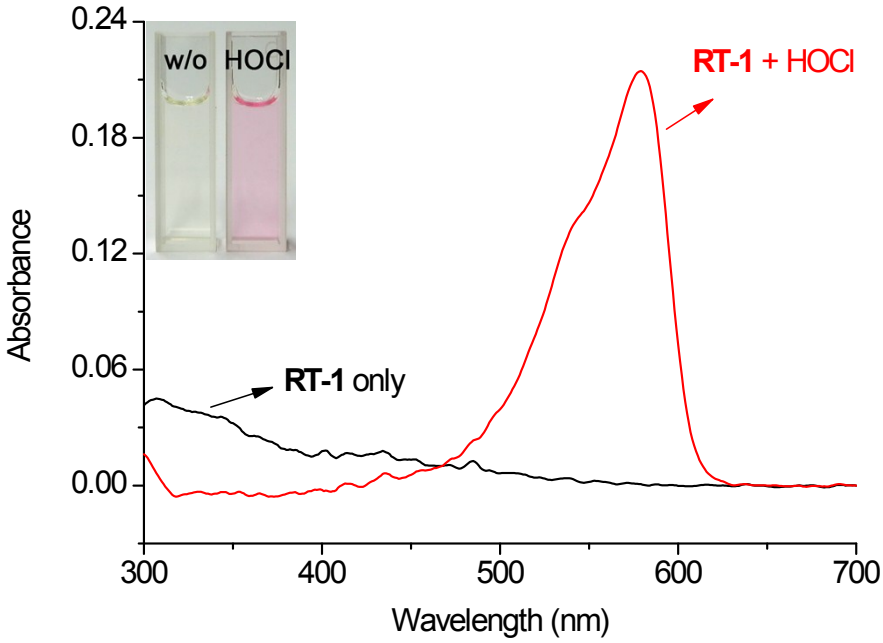

Fig. S2. UV–vis spectra of **RT-1** in the presence and absence of HOCl. [**RT-1**] = 5.0 × 10^{-6} M, [HOCl] = 5.0 × 10^{-5} M in phosphate buffer solution (pH 7.4) containing 1% (*v/v*) acetonitrile.

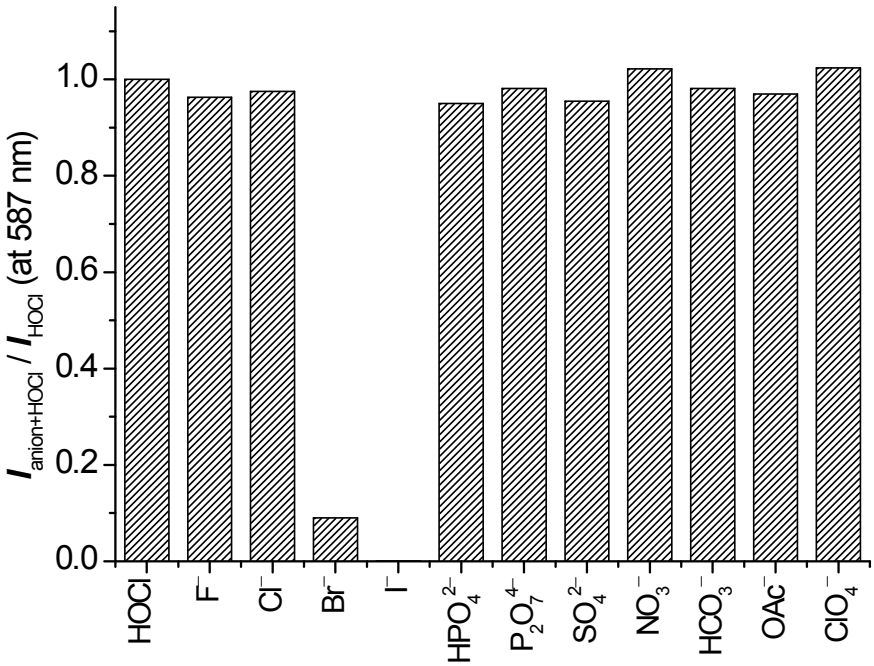

Fig. S3. Competitive signaling of HOCl by **RT-1** in the presence of common anions as a background. [**RT-1**] = 5.0 × 10^{-6} M, [HOCl] =2.5 × 10^{-5} M, [A^{n-}] = 5.0 × 10^{-5} M in phosphate buffer solution (pH 7.4) containing 1% (*v/v*) acetonitrile, λ_{ex} = 550 nm.

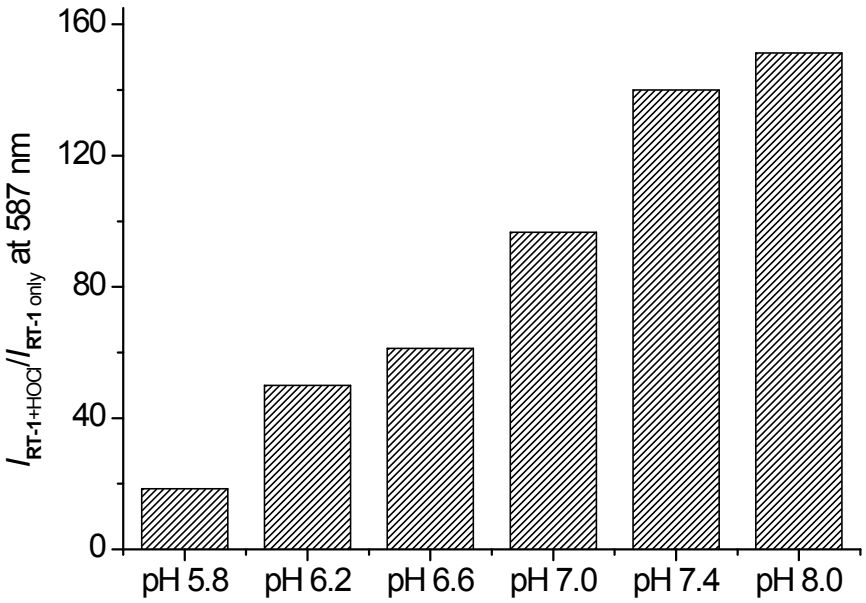

Fig. S4. Effect of pH on HOCl signaling by **RT-1**. [**RT-1**] = 5.0 × 10^{-6} M, [HOCl] = 2.5 × 10^{-5} M in phosphate buffer solution containing 1% (*v/v*) acetonitrile, λ_{ex} = 550 nm.

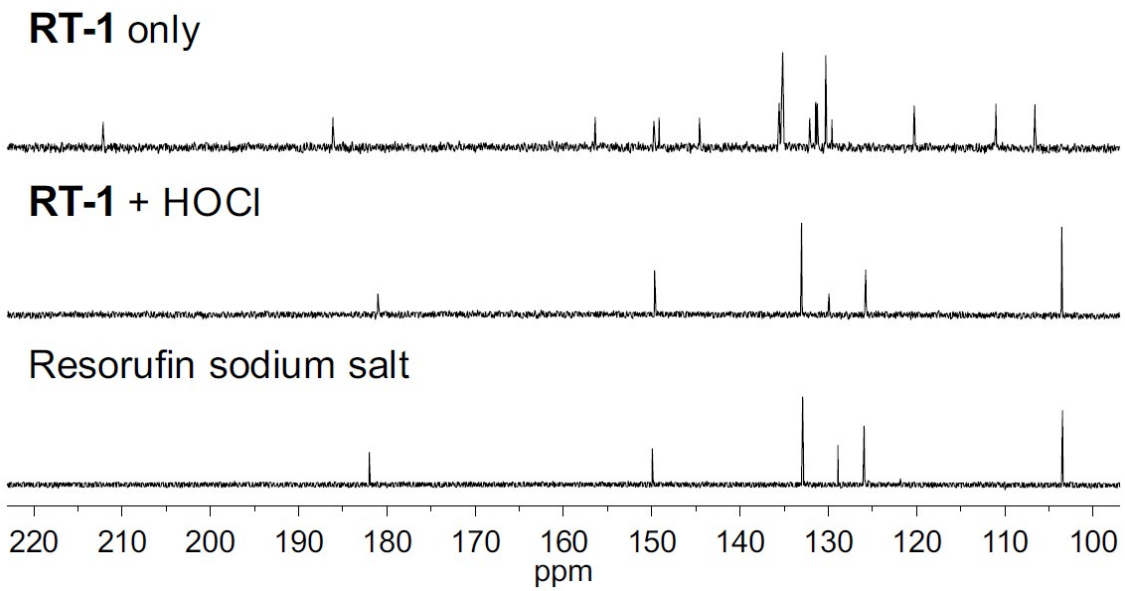

Fig. S5. Partial ^{13}C NMR spectra of **RT-1**, **RT-1** + HOCl, and resorufin sodium salt. [**RT-1**] = [resorufin sodium salt] = 1.0 × 10^{-2} M in DMSO-d_6. Middle NMR spectrum (**RT-1** + HOCl) was obtained after purification of the reaction product of **RT-1** and HOCl (1.1 eq) using a short silica column.

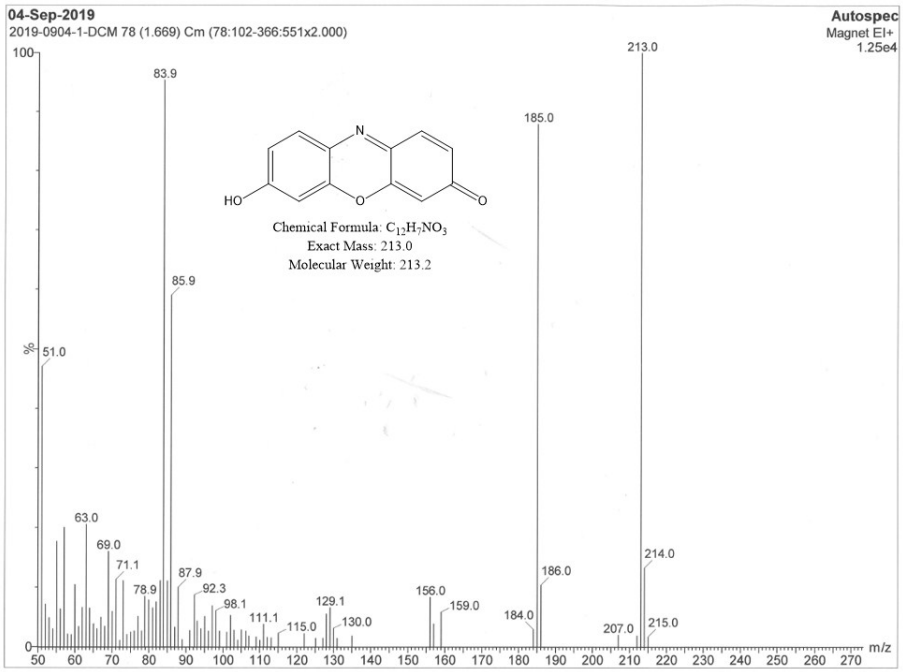

Fig. S6. EI (direct injection probe) mass spectrum of the HOCl signaling product of **RT-1**.

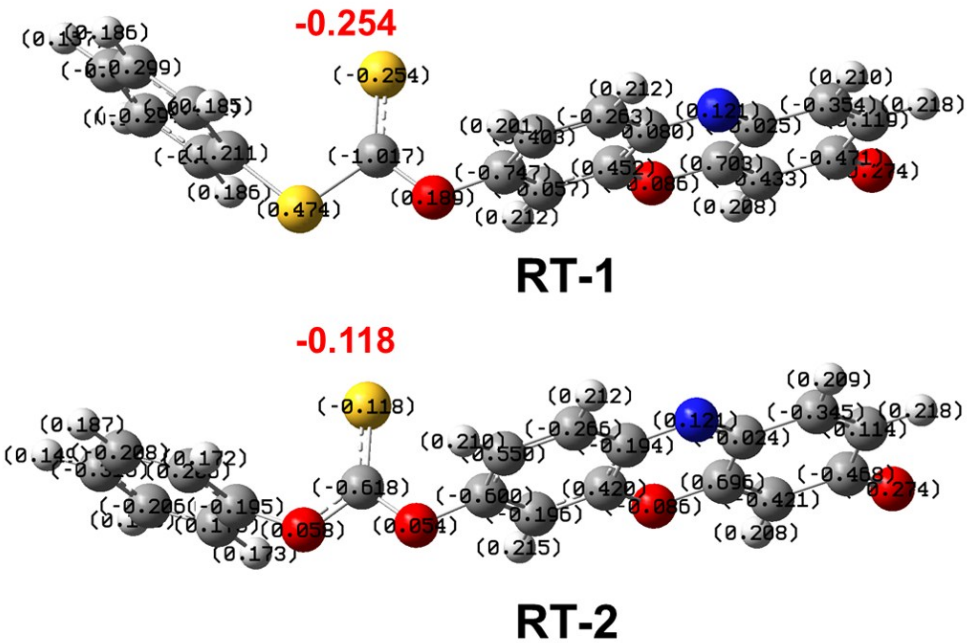

Fig. S7. Mulliken charge distribution of **RT-1** and **RT-2**.

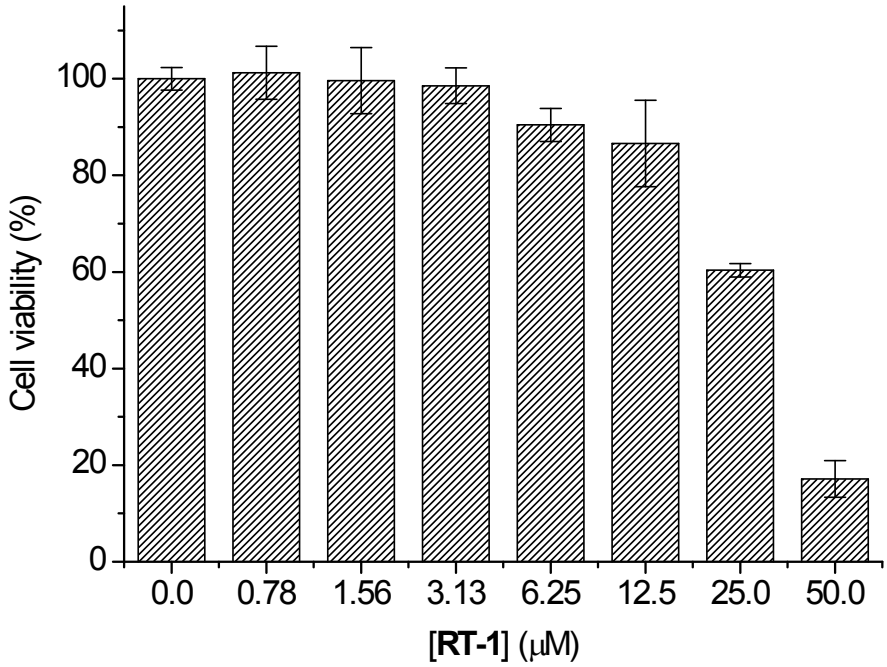

Fig. S8. MTT assay of **RT-1** in HeLa cells. [**RT-1**] = 0–5.0 × 10^{-5} M.

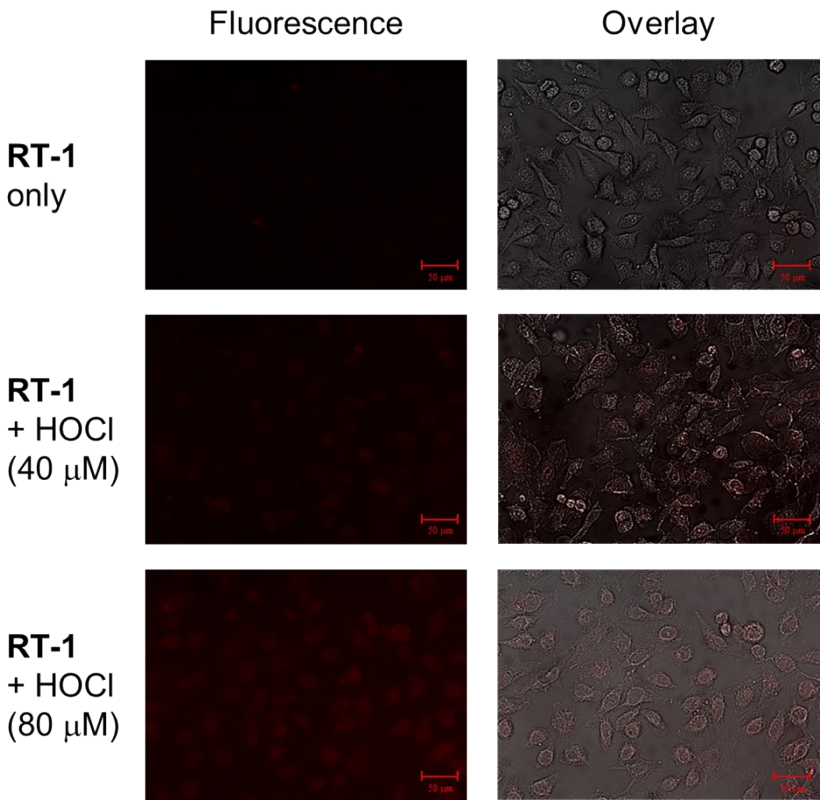

Fig. S9. Confocal microscopy images of HeLa cells stained with 3.0 μM of **RT-1** in the presence (40 μM, 80 μM) and absence of HOCl.

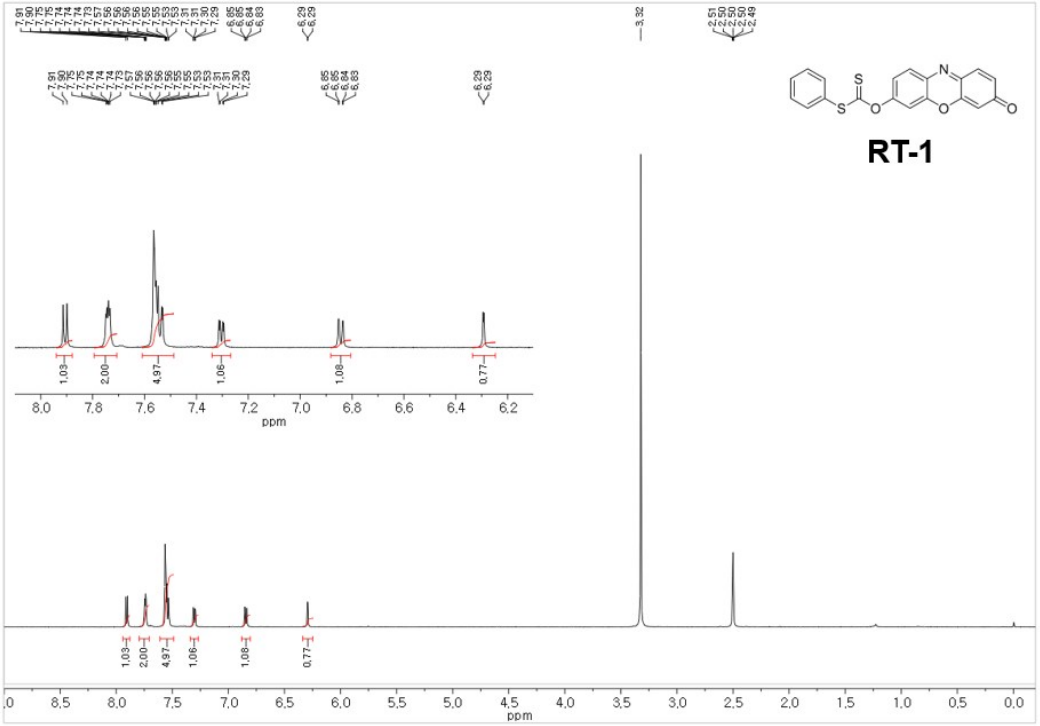

Fig. S10. ^{1}H NMR spectrum of **RT-1** in DMSO-d_6 (600 MHz).

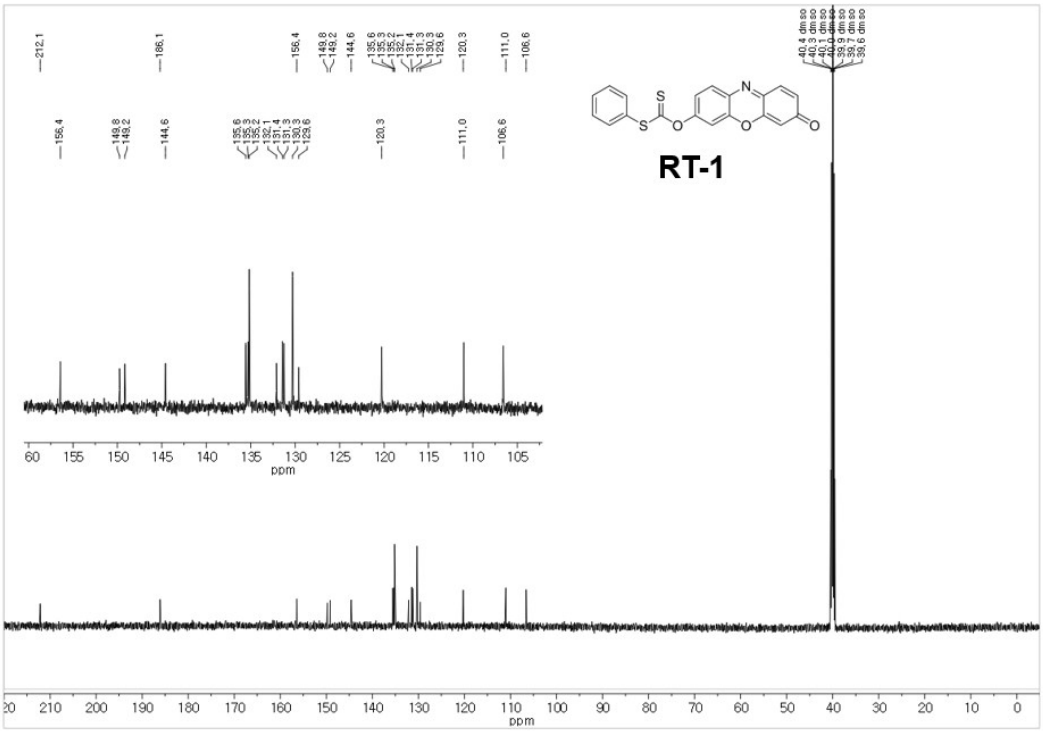

Fig. S11. ^{13}C NMR spectrum of **RT-1** in DMSO-d_6 (150 MHz).

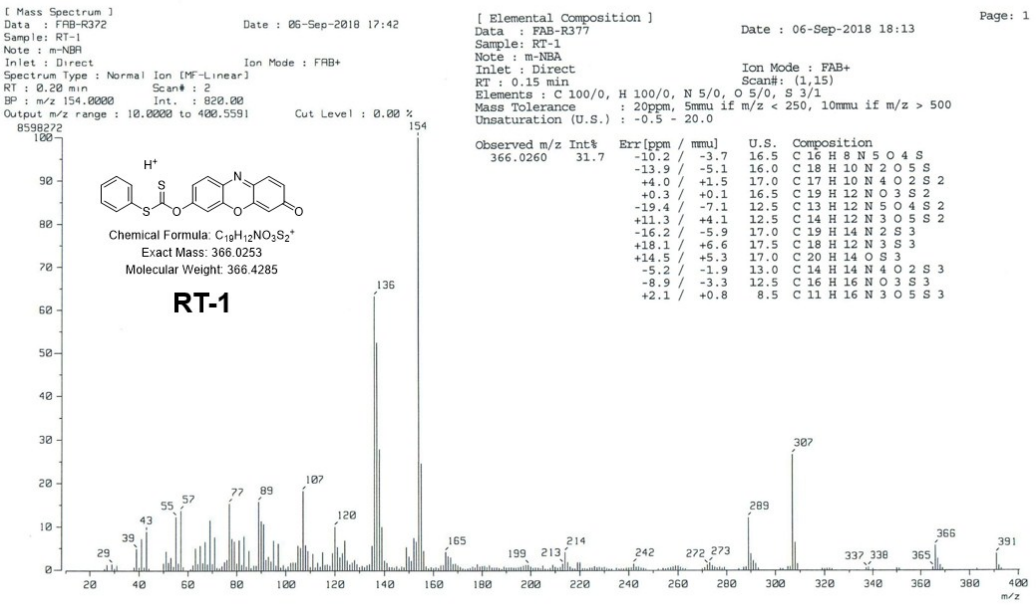

Fig. S12. High-resolution FAB mass spectrum of **RT-1**.

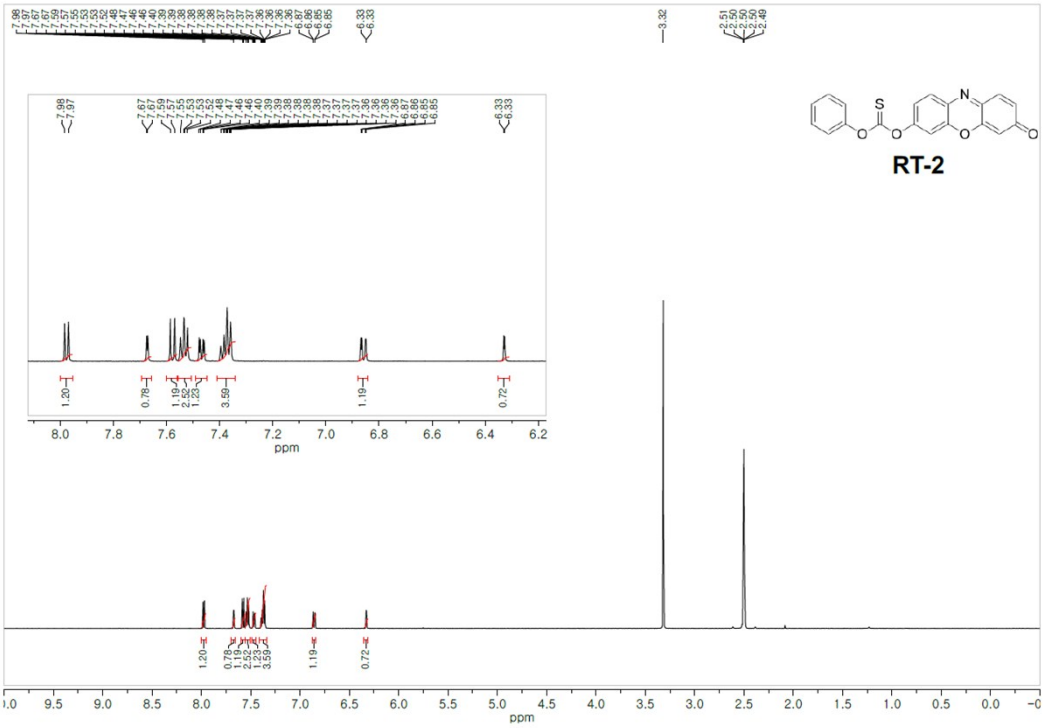

Fig. S13. ^{1}H NMR spectrum of **RT-2** in DMSO-d_6 (600 MHz).

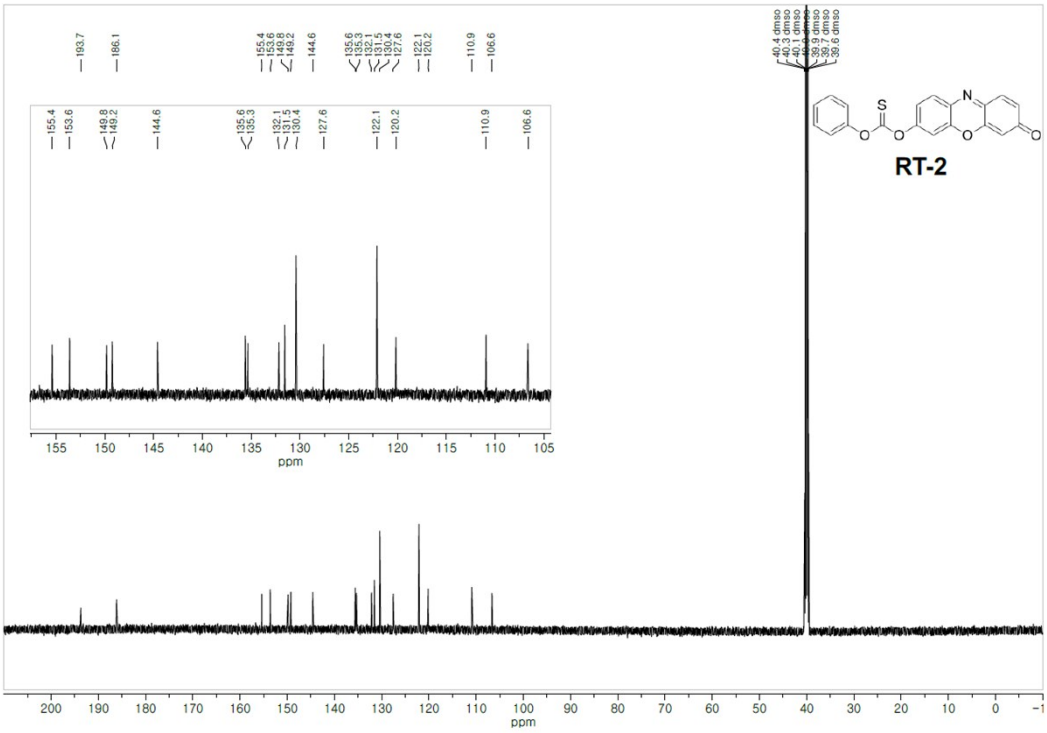

Fig. S14. ^{13}C NMR spectrum of **RT-2** in DMSO-d_6 (150 MHz).

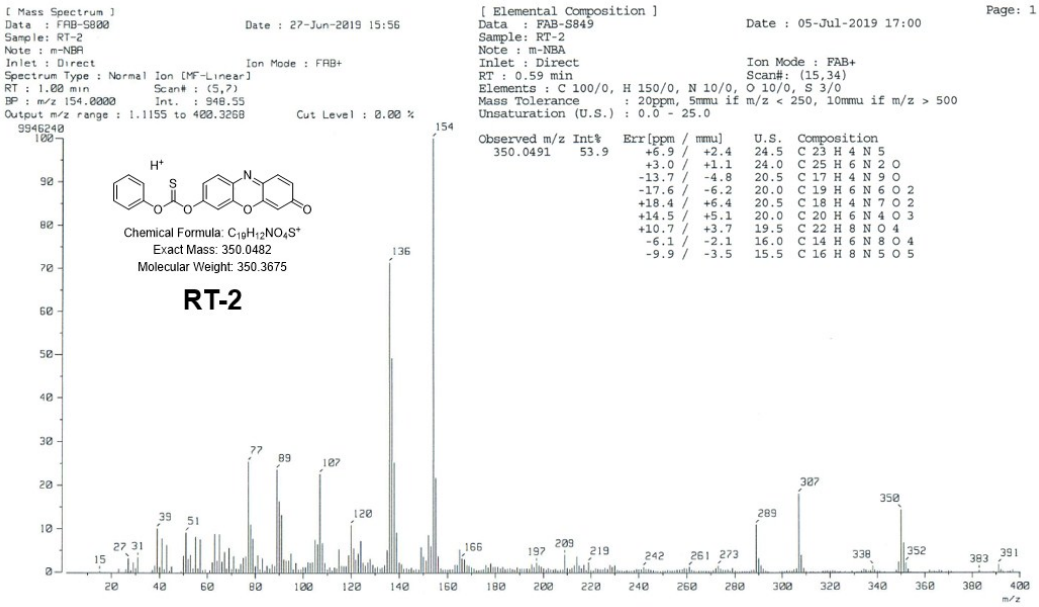

Fig. S15. High-resolution FAB mass spectrum of **RT-2**.

References:

[1] Y. K. Yang, H. J. Cho, J. Lee, I. Shin and J. Tae, *Org. Lett.*, 2009, **11**, 859–861.

[2] L. Qiao, H. Nie, Y. Wu, F. Xin, C. Gao, J. Jing and X. Zhang, *J. Mater. Chem. B*, 2017, **5**, 525–530.

[3] B. Wang, D. Chen, S. Kambam, F. Wang, Y. Wang, W. Zhang, J. Yin, H. Chen and X. Chen, *Dyes Pigment.*, 2015, **120**, 22–29.

[4] S. I. Reja, V. Bhalla, A. Sharma, G. Kaur and M. Kumar, *Chem. Commun.*, 2014, **50**, 11911–11914.

[5] Q. Wang, C. Liu, J. Chang, Y. Lu, S. He, L. Zhao and X. Zeng, *Dyes Pigment.*, 2013, **99**, 733–739.

[6] X. Chen, K.-A. Lee, E.-M. Ha, K. M. Lee, Y. Y. Seo, H. K. Choi, H. N. Kim, M. J. Kim, C.-S. Cho, S. Y. Lee, W.-J. Lee and J. Yoon, *Chem. Commun.*, 2011, **47**, 4373–4375.

[7] S. Ding, Q. Zhang, S. Xue and G. Feng, *Analyst*, 2015, **140**, 4687–4693.

[8] L. Yuan, L. Wang, B. K. Agrawalla, S.-J. Park, H. Zhu, B. Sivaraman, J. Peng, Q.-H. Xu and Y.-T. Chang, *J. Am. Chem. Soc.*, 2015, **137**, 5930−5938.

[9] Y. Jiang, G. Zheng, Q. Duan, L. Yang, J. Zhang, H. Zhang, J. He, H. Sun and D. Ho, *Chem. Commun.*, 2018, **54**, 7967–7970

[10] L. Wu, Q. Yang, L. Liu, A. C. Sedgwick, A. J. Cresswell, S. D. Bull, C. Huang and T. D. James, *Chem. Commun.*, 2018, **54**, 8522–8525.

[11] Y. L. Pak, S. J. Park, D. Wu, B. Cheon, H. M. Kim, J. Bouffard and J. Yoon, *Angew. Chem. Int. Ed.*, 2018, **57**, 1567–1571.